ISSN 1064-2269, Journal of Communications Technology and Electronics, 2006, Vol. 51, No. 5, pp. 534–544. © Pleiades Publishing, Inc., 2006.
Original Russian Text © D.A. Smirnov, 2006, published in Radiotekhnika i Elektronika, 2006, Vol. 51, No. 5, pp. 569–579.

STATISTICAL RADIO PHYSICS

Characterization of Weak Coupling between Self-Oscillation Systems from Short Time Series: Technique and Applications

D. A. Smirnov

Received December 19, 2005

Abstract—A technique is developed for characterizing the coupling of self-oscillation systems from observable signals (time series). The technique is based on the empirical modeling of phase dynamics in such systems and extended to the case of short time series and high noise levels. Corrections to the conventional estimates are introduced to eliminate their systematic errors, and formulas for the confidence intervals are derived. The effectiveness and applicability of the technique are demonstrated by numerical experiments and examples from neurophysiology and climatology: an increased influence of the pathological focus on adjacent brain regions is detected in the intracranial electroencephalograms of a patient with temporal lobe epilepsy as a precursor of a seizure, and the influence of the El Niño–Southern Oscillation phenomenon on the North Atlantic Oscillation is revealed from the records of the climate indexes (sea-surface temperature and atmospheric pressure).

PACS numbers: 05.45.Tp

DOI: 10.1134/S106422690605007X

INTRODUCTION

The analysis of couplings (their presence, strength, and "directionality patterns") between oscillatory systems is necessary in various fields of science and practice, including radio physics [1], climatology [2], cardiology [3–5], and medical diagnostics of neurophysiological processes [6, 7]. In many cases, such information can only be extracted from empirically obtained signals. Characterization of coupling has practical significance. For example, revealing the cause-and-effect relationships between global climatic processes is important for understanding their mechanisms and the causes of global climate change. Localization of epileptic foci by analyzing the interaction between different brain regions with the use of electro- and magnetoencephalograms [6–8] is one of the potential applications.

The essential nonstationarity of processes (typical of biological objects) and the impossibility to accumulate a large body of data (typical of geophysics) necessitate the characterization of coupling from short time series. The problem is complicated further by the presence of noise, especially if the coupling is weak. In this study, a method is developed for estimating the coupling between two self-oscillation systems with the use of relatively short time series (as short as 30–50 oscillation periods).

Sufficiently strong couplings are detectable by linear methods, such as the cross-correlation function, the coherence function, and the cross-wavelet spectra. However, to analyze nonlinear self-oscillation systems, it is better to use nonlinear techniques, which are more sensitive to weak couplings. One of such methods relies on the empirical modeling of the phase dynamics of investigated oscillators [9]. This technique permits not only detection of coupling between the oscillators but also estimation of the strength of their mutual influence (see Section 1).

This technique is effective for sufficiently long time series (1000 characteristic periods or more) in the presence of moderate noise [10]. However, estimates based on a series consisting of several tens of cycles not only exhibit a high level of fluctuations (high probability of erroneous determination of the coupling character) but can also appear to be biased, i.e., to contain systematic errors (see Section 1). In this study, the statistical properties of such estimates are analyzed in detail, corrections for their systematic errors are proposed, and the confidence intervals ensuring a low level of random erroneous decisions are defined (Section 2). Formulas for the confidence intervals are derived analytically for linear uncoupled processes, and their applicability to moderately nonlinear weakly coupled systems is demonstrated numerically. Examples of their application in neurophysiology and climatology are presented in Sections 3 and 4.

1. ESTIMATION OF COUPLING VIA PHASE DYNAMICS MODELING

The main idea of the method is to estimate the extent to which the current phase of one of the oscillation systems influences the following evolution of the phase in

the other system. To do this, initial time series of the two oscillators $\{x_1(t_1), \ldots, x_1(t_{N_x})\}$ and $\{x_2(t_1), \ldots, x_2(t_{N_x})\}$ (where $t_i = i\Delta t$, Δt is the sampling interval and N_x is the series length) are used to calculate time series of the oscillation phases $\{\varphi_1(t_1), \ldots, \varphi_1(t_N)\}$ and $\{\varphi_2(t_1), \ldots, \varphi_2(t_N)\}$. On the basis of the series thus obtained, an empirical model is constructed [9], and the model coefficients are used to estimate the characteristics of coupling.

1A. Calculation of Phase

The classical method to determine the phase of a signal $X(t)$ is to calculate complex analytic signal $Z(t) = X(t) + jY(t)$, where Y is the Hilbert transform of the initial signal [11]. Phase $\varphi(t)$ is determined as the argument of $Z(t)$, i.e., the rotation angle of the radius vector on the complex plane (ReZ, ImZ). Hereafter, we deal with unwrapped phase $\varphi(t)$ that increases by 2π in each complete revolution of the radius vector. Phase determined via the Hilbert transform has a clear physical meaning only for signals with a pronounced main rhythm. If signal $X(t)$ is wideband, it is subjected to bandpass filtering and the above procedure is applied to the filtered signal. However, physical justification of the selected passband is required. In any case, the values of phase at the ends of a time series are ill defined (edge effect) and should be omitted over approximately ten oscillation periods from both ends [12].

When relatively short series are analyzed, it is preferable to construct the analytic signal according to an approach [13] that is equivalent to bandpass filtering followed by the Hilbert transform but less prone to edge effects. This approach is based on the complex wavelet transform

$$Z(t) = \frac{1}{\sqrt{s}}\int_{-\infty}^{\infty} X(t')\psi^*((t-t')/s)dt', \qquad (1)$$

where the complex wavelet function is taken in the form of the Morlet wavelet $\psi(\eta) = \pi^{-1/4}\exp(-j\omega_0\eta) \times \exp(-\eta^2/2)$, the asterisk denotes complex conjugation, and s is a fixed time scale. As before, the phase is defined as an argument of $Z(t)$. Here, in fact, signal X passes through a bandpass filter with the center frequency $f \approx \dfrac{\omega_0}{2\pi s}$ and the bandwidth controlled by parameter ω_0. For example, at $\omega_0 = 6$, the bandwidth is approximately one-quarter of the center frequency $f \approx 1/s$ and the edge effects take place within the intervals of length $\sqrt{2}\,s$ [13, 14].

1B. Characteristics of Coupling

The mathematical model of phase dynamics is chosen from the following considerations. In many situations, phase dynamics of oscillators with a pronounced main rhythm is adequately described by the stochastic differential equations [15]

$$d\varphi_{1,2}/dt = \omega_{1,2} + G_{1,2}(\varphi_{1,2}, \varphi_{2,1}) + \xi_{1,2}(t), \qquad (2)$$

where parameters ω_k determine circular frequencies of oscillations and $\xi_k(t)$ are independent Gaussian white noises with the zero mean and autocorrelation functions $\langle\xi_k(t)\xi_k(t')\rangle = 2D_k\delta(t-t')$. For the analysis of discrete time series, the equation is represented in the difference form

$$\begin{aligned}&\varphi_{1,2}(t+\tau) - \varphi_{1,2}(t)\\ &= F(\varphi_{1,2}(t), \varphi_{2,1}(t), \vec{a}_{1,2}) + \varepsilon_{1,2}(t),\end{aligned} \qquad (3)$$

where τ is a finite time interval; $\varepsilon_k(t)$ are zero-mean noises; and F is the trigonometric polynomial

$$\begin{aligned}F(\varphi_1, \varphi_2, \vec{a}_k) &= \frac{\alpha_0^{(k)}}{\sqrt{2}} + \sum_{m,n}(\alpha_{m,n}^{(k)}\cos(m\varphi_1 + n\varphi_2)\\ &+ \beta_{m,n}^{(k)}\cos(m\varphi_1 + n\varphi_2)), \quad k = 1, 2,\end{aligned} \qquad (4)$$

where $\vec{a}_k \equiv \{a_{k,j}\} \equiv (\alpha_0^{(k)}, \{\alpha_{m,n}^{(k)}\}, \{\beta_{m,n}^{(k)}\})$ are the vectors of coefficients. If the "true" equations of phase dynamics in the form (2) or (3) are known a priori, the degree of influence exerted by the second oscillator on the first one (c_1) can be determined by the slope of dependence $F(\varphi_1, \varphi_2, \vec{a}_1)$ on φ_2. By analogy, expressing the influence of the first oscillator on the second (c_2), we have

$$c_{1,2}^2 = \frac{1}{2\pi^2}\int_0^{2\pi}\int_0^{2\pi}(\partial F(\varphi_{1,2}, \varphi_{2,1}, \vec{a}_{1,2})/\partial\varphi_{2,1})^2 d\varphi_1 d\varphi_2.$$

Characteristics $c_{1,2}^2$ can be expressed in terms of the polynomial coefficients (4) as

$$c_k^2 = \sum_j n_j^2 a_{k,j}^2, \qquad (5)$$

where n_j is the value of n in the trigonometric monomial corresponding to coefficient $a_{k,j}$. The normalized index of coupling directionality is introduced as $d = (c_2 - c_1)/(c_2 + c_1)$ and takes values over the interval $[-1, 1]$. If $d = 1$ or -1, the coupling is unidirectional (only the influence $1 \longrightarrow 2$ or $2 \longrightarrow 1$, respectively), while the case of $d = 0$ corresponds to symmetric coupling. In

other cases, the sign of d indicates the predominant direction of coupling.

1C. Estimated Characteristics of Coupling

In practice, a time series is given and the equations of phase dynamics are unknown. Therefore, the problem is to estimate coupling characteristics c_1, c_2, and d from the known time series. To do this, the time series of phases are calculated and empirical model (3) and (4) is constructed. Interval τ is taken equal to the characteristic oscillation period. Coefficients $\hat{\vec{a}}_k$ are calculated by the least squares routine (LSR), i.e., from the condition

$$\sum_{i=1}^{N-\tau/\Delta t} \varphi_{1,2}(t_i+\tau) - \varphi_{1,2}(t_i) - F(\varphi_{1,2}(t_i), \varphi_{2,1}(t_i), \hat{\vec{a}}_{1,2}))^2 \longrightarrow \min. \quad (6)$$

The degrees of the mutual influence of the oscillators are estimated from (5) by substituting the found values of $\hat{\vec{a}}_k$ for the true values of $\vec{a}_k$.

The above technique is unsuitable for a pair of phase-locked oscillators because their phases cannot be taken as independent variables of the model in this case. Phase locking manifests itself when phase coherence factor $\rho \equiv |\langle \exp(j(\varphi_1(t) - \varphi_2(t)))\rangle|$ (angle brackets denotes time averaging) is close to unity [7], while the technique fails as early as at $\rho > 0.6$ [1].

1D. Properties of the Estimated Characteristics of Coupling

Under certain general conditions, estimates $\hat{\vec{a}}_k$ are consistent [16]; i.e., the probability of their noncoincidence with true values tends to zero for a very long series ($N \longrightarrow \infty$). Therefore, estimates $\hat{c}_{1,2}$ and $\hat{d}$ also closely coincide with the true values of $c_{1,2}$ and d, a result that allows a correct conclusion to be drawn about coupling [9]. However, it is a priori unknown whether a time series is sufficiently long. In the case it is not, estimates $\hat{c}_{1,2}$ and $\hat{d}$ may appear to be biased and the statistical significance of this bias has to be calculated.

Let us illustrate the importance of this problem by a simple demonstrative example. Consider uncoupled and linear oscillators, which are described by Eqs. (2) with $G_{1,2} \equiv 0$. Analytic integration of (2) over interval τ yields

$$\varphi_k(t+\tau) - \varphi_k(t) = \omega_k\tau + \varepsilon_k(t), \quad (7)$$

where $\varepsilon_k(t)$ are independent Gaussian random processes with variances $2D_k\tau$. In this case, $c_1 = c_2 = d = 0$, while their estimated values $\hat{c}_{1,2}$ and $\hat{d}$ are misleading (Figs. 1a, 1b).

Figure 1 presents the distributions of estimates obtained in the numerical experiments. Here and below, the experimental procedure was as follows. An ensemble comprising 1000 time series of length $N = 1000$ was generated by sampling with the interval $\Delta t = 0.2\pi$. For the used values $\omega_1 = \omega_2 = 1$, the characteristic oscillation period contains ten points. Each of the time series was obtained via the numerical integration of Eqs. (2) using the Euler algorithm with the step $h = 0.01\pi$. The

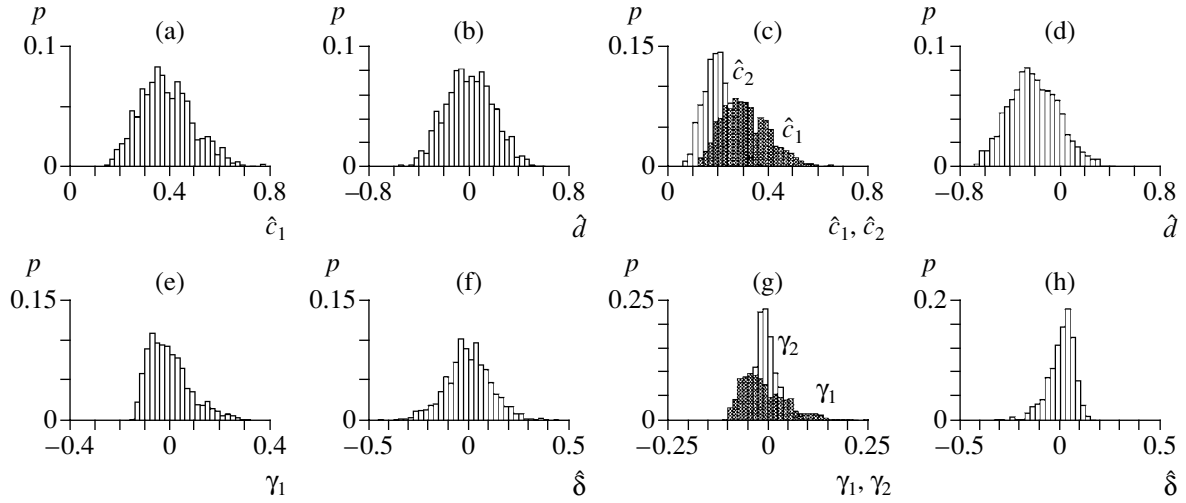

Fig. 1. Histograms of the coupling parameters estimated over an ensemble of time realizations (7) for (a, b, e, f) $D_1 = D_2 = 0.2$ and (c, d, g, h) $D_1 = 0.2$ and $D_2 = 0.05$.

initial values of phases, $\varphi_1(0)$ and $\varphi_2(0)$, were randomly chosen from the interval $[0, 2\pi]$. For each series, model equations (3) and (4) were constructed with $\tau = 2\pi$ and the third-order polynomials including the terms with $m = 0, \ldots, 3$, $n = 0$; $n = 1, \ldots, 3$, $m = 0$; and $m, n = \pm 1$. Such a structure is fairly compact. Furthermore, the structure allows the description of nontrivial nonlinearities because it comprises a number of harmonics [9]. The estimated characteristics were calculated and the sets of 1000 values were used to calculate their distributions, mean values, variances, and the number of correct and erroneous conclusions on the presence of coupling.

In the case of identical oscillators ($D_1 = D_2$), $\hat{c}_1$ is positive and considerably large (Fig. 1a); hence, it gives a biased estimate for $c_1 = 0$. Estimate $\hat{d}$ is unbiased but varies over a wide range: values up to ± 0.4 are often encountered (Fig. 1b). This means that the probability of making an erroneous decision about the presence of interaction between the oscillators is high when a single time realization is used. The situation becomes ever more complicated for nonidentical oscillators (e.g., $D_1 > D_2$ in Figs. 1c, 1d). Estimates $\hat{c}_{1,2}$ are biased, with $\hat{c}_1$ being biased to a greater degree (Fig. 1c). Because of this circumstance, estimate $\hat{d}$ is systematically less than zero (Fig. 1d). This finding suggests a predominant influence in the direction $2 \longrightarrow 1$, whereas the oscillators are actually uncoupled. For oscillators with different oscillation frequencies (at $\tau > \Delta t$), estimates $\hat{c}_1$ and $\hat{c}_2$ also have unequal biases. Let us dwell on the cause of these errors.

Since $\hat{c}_{1,2}$ and $\hat{d}$ are functions of estimates $\hat{\hat{a}}_k$, their probabilistic properties can be derived from the known properties of $\hat{\hat{a}}_k$, which in turn depend on the properties of noise ε_k. Let estimates $\hat{\hat{a}}_k$ be unbiased (see Appendix). Then, in accordance with the probability theory, mathematical expectation of each estimate $\hat{a}_{k,j}$ can be represented as $M[\hat{a}_{k,j}^2] = a_{k,j}^2 + \sigma_{k,j}^2$, where M is the mean and $\sigma_{k,j}^2$ is the variance of estimate $\hat{a}_{k,j}$. Thus, $\hat{a}_{k,j}^2$ is a biased estimate of $a_{k,j}^2$ and its bias is equal to $\sigma_{k,j}^2$. Taking into account formula (5), we obtain

$$M[\hat{c}_k^2] = \sum_j n_j^2 M[\hat{a}_{k,j}^2] = c_k^2 + \sum_j n_j^2 \sigma_{k,j}^2, \qquad (8)$$

whence it is seen that $\hat{c}_k^2$ is a biased estimate of c_k^2, although estimates $\hat{a}_{k,j}$ are unbiased. The bias c_k^2 is equal to $\sum_j n_j^2 \sigma_{k,j}^2$. As the variance of noise ε_k increases and the time series decreases, the bias increases because of the similar dependence of variances $\sigma_{k,j}^2$ on these variables (see Appendix). Hence, for short series, $\hat{c}_k^2$ is systematically greater than c_k^2. This fact is illustrated in Fig. 1a.

Since the values of $\sigma_{k,j}^2$ grow with increasing D_k, the bias in $\hat{c}_1$ exceeds the bias in $\hat{c}_2$ for $D_1 > D_2$ and other conditions being equal. This result is well seen in Fig. 1c. The values of $\sigma_{k,j}^2$ grow with increasing ω_k as well (see Appendix), a circumstance that explains the aforementioned unequal bias in $\hat{c}_1$ and $\hat{c}_2$ for uncoupled oscillators with different circular frequencies.

2. COUPLING ESTIMATES FOR SHORT-TIME SERIES

2A. Derivation of Formulas

Let us find confidence intervals for c_k^2. For this purpose, we take estimate $\hat{c}_k^2$ as a base and eliminate its bias. According to (8), the unbiased estimate of c_k^2 is

$$\gamma_k = \hat{c}_k^2 - \sum_j n_j \hat{\sigma}_{k,j}^2, \qquad (9)$$

where $\hat{\sigma}_{k,j}^2$ are the unbiased estimates of $\sigma_{k,j}^2$. In the general case, no analytic expression for $\hat{\sigma}_{k,j}^2$ can be obtained. However, this can be done by simplifying assumptions on the properties of noises $\varepsilon_k(t)$, which are assumed to be Gaussian and independent of both each other and $\varphi_{1,2}(t)$. The derived estimates $\hat{\sigma}_{k,j}^2$ are complicated functions of τ and $\hat{a}_{k,1}$ (see Appendix, formula (A.3)).

Quantities γ_k characterize the presence of coupling between the oscillators. Characterization of the coupling direction by normalized directionality d leads to difficulties in the following analysis. It is convenient to use the quantity $\delta = c_2^2 - c_1^2$ instead, whose unbiased estimate is $\hat{\delta} = \gamma_2 - \gamma_1$.

The goal now is to determine the significance of estimates γ_k and $\hat{\delta}$ obtained from a single realization. For the time series under study (with $N \approx 10^3$ and ten points for the characteristic period), the variance of γ_k (9) approximately equals the variance of estimate

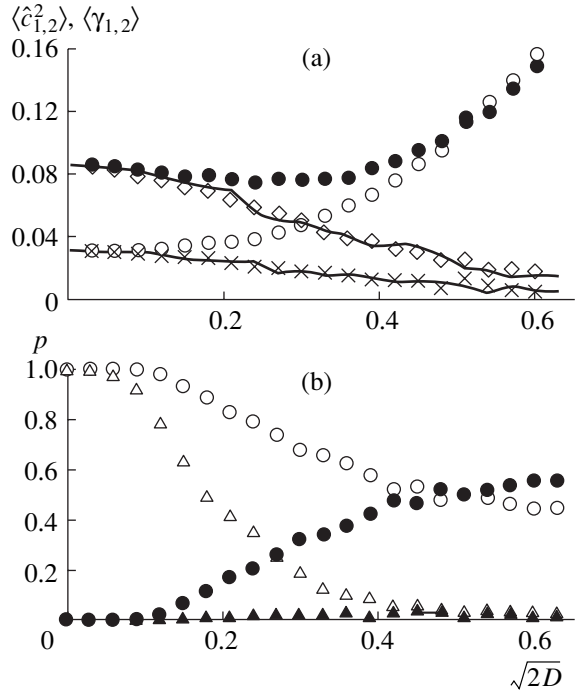

Fig. 2. Properties of the coupling parameters for time realizations (2) with nonlinear functions $G_{1,2}$: (a) ensemble-averaged values of (open circles) $\hat{c}^2_1$, (closed circles) $\hat{c}^2_2$, (crosses) γ_1, (diamonds) γ_2, and (solid lines) close-to-ideal values of $c^2_{1,2}$ calculated from a long time series and (b) the rates of making correct and erroneous decisions on the direction of coupling on the basis of (open and closed circles, respectively) estimate $\hat{d}$ and (open and closed triangles, respectively) $\hat{\delta}$.

$\hat{c}^2_k$ (see Appendix) and can be expressed in terms of the covariances of $\hat{a}_{k,j}$:

$$\sigma^2_{\gamma_k} \approx \sum_{i,j} n_i^2 n_j^2 \mathrm{cov}(\hat{a}^2_{k,i}, \hat{a}^2_{k,j}). \quad (10)$$

Since the true values of the covariances are unknown, they need to be estimated. Thus, obtainment of a "good" estimate $\hat{\sigma}^2_{\gamma_k}$ for $\sigma^2_{\gamma_k}$ is difficult owing to the following circumstances. On the one hand, it is necessary to eliminate the undervalued estimates of $\sigma^2_{\gamma_k}$ in order to diminish the number of erroneous conclusions about the type of coupling. On the other hand, these estimates cannot be overvalued if the presence of mutual influence is to be detected. As a result, a trade-off semiempirical formula (A.4) was derived.

In the case of low-order polynomials F used in this study, the distribution of γ_k is asymmetric. Hence, it is reasonable to take the confidence interval for c^2_k in the asymmetric form $[\gamma_k - R_1\hat{\sigma}_{\gamma_k}, \gamma_k + R_2\hat{\sigma}_{\gamma_k}]$. Constants R_1 and R_2 were fit empirically from numerical experiments with system (7) to ensure the required level of confidence. For example, for third-order polynomials F, the 95% confidence interval corresponds to $R_1 = 1.6$ and $R_2 = 1.8$. The presence of influence on the kth oscillator can be inferred with an error probability of 0.025 if

$$\gamma_k - R_1\hat{\sigma}_{\gamma_k} > 0. \quad (11)$$

To determine the directionality of coupling, we should find the variance of $\hat{\delta}$, whose unbiased estimate is $\hat{\sigma}^2_\delta = \hat{\sigma}^2_{\gamma_1} + \hat{\sigma}^2_{\gamma_2}$. Since $\hat{\delta}$ is usually distributed almost symmetrically, the confidence interval for δ is taken in the symmetric form $\hat{\delta} \pm R\hat{\sigma}_{\hat{\delta}}$. The experiments show that a 95% confidence interval is achieved for $R = 1.6$. If the obtained estimates satisfy the inequalities

$$\gamma_2 - R_1\hat{\sigma}_{\gamma_2} > 0 \text{ and } \hat{\delta} - R\hat{\sigma}_{\hat{\delta}} > 0, \quad (12)$$

the predominant influence $1 \longrightarrow 2$ can be inferred with an error probability of 0.025. Conversely, if

$$\gamma_1 - R_1\hat{\sigma}_{\gamma_1} > 0 \text{ and } \hat{\delta} + R\hat{\sigma}_{\hat{\delta}} < 0, \quad (13)$$

the influence $2 \longrightarrow 1$ dominates with the same error probability. If neither of conditions (12) or (13) is valid, the coupling directionality cannot be determined with a required level of reliability.

2B. Numerical Testing of the Estimates

Let us first consider the results of using proposed new estimates γ_k and $\hat{\delta}$ in the example described in Section 1D. Systematic errors are absent in all cases of using estimates γ_k and $\hat{\delta}$, as illustrated in Figs. 1e–1h. According to expectations, the false detection rate in detecting the coupling $1 \longrightarrow 2$ by formula (11) was 0.025. The fractions of errors in the predominant coupling direction determined on the basis of (12) and (13) were also close to 0.025, and the total rate of mistaking the coupling direction was 0.05. These results suggest that the new estimates are unbiased and the percentage of random errors is adequately controlled. This result comes as no surprise because all formulas for the new estimates were derived precisely for the case of system (2) with $G_{1,2} \equiv 0$.

The following numerical experiment was performed to demonstrate that the new estimates are also applicable when functions $G_{1,2}$ in (2) take nonzero yet small values. Now, let the time series be generated by system (2) with $G_1(\varphi_1, \varphi_2) = 0.03\sin(\varphi_2 - \varphi_1)$, $G_2(\varphi_2, \varphi_1) = 0.05\sin(\varphi_1 - \varphi_2)$, $\omega_1 = 1.1$, $\omega_2 = 0.9$, and $D_1 = D_2 = D$. In

this case, the assumptions used to derive the expressions for the new estimates are slightly infringed owing to the nonlinearity of functions $G_{1,2}$.

Figure 2a plots the dependences of ensemble-averaged estimates $\langle \hat{c}_k^2 \rangle$ and $\langle \gamma_k \rangle$ on the noise level $\sqrt{2D}$ ranging from 0 to 0.63. The true values of c_k^2 are unknown; instead, the "almost true" values calculated from a very long time series ($N = 2 \times 10^5$) are shown (solid lines). It is seen that the biases of estimates $\hat{c}_k^2$ grow with an increase in the noise level. For example, at $\sqrt{2D} = 0.6$, $\hat{c}_k^2$ is greater than c_k^2 by a factor of 20. As regards estimate γ_k, it is practically unbiased for any noise level.

Figure 2b plots the rates of correct and erroneous decisions about the coupling direction (p) obtained on the basis of $\hat{d}$ and $\hat{\delta}$. At the high noise level $\sqrt{2D} = 0.6$, the sign of $\hat{d}$ leads to an erroneous decision in more than half of the cases. At the same noise level, the number of erroneous decisions made while checking the validity of (12) and (13) is 20 (at an expected error probability of 0.025) and the number of correct decisions is 24. For the rest of the realizations, only a conservative conclusion that neither of the coupling directions can be reliably considered as dominant is drawn. In other words, at $\sqrt{2D} = 0.6$, a time series of $N = 1000$ points is not long enough to provide for reliable determination of the coupling direction.

As the noise level drops, the number of erroneous decisions decreases and the number of correct decisions increases, whether estimate $\hat{d}$ or $\hat{\delta}$ is used. However, the rate of making an error with the use of $\hat{d}$ is considerable, 10–20%, even at the relatively low noises $0.1 \le \sqrt{2D} \le 0.2$. In the case of $\hat{\delta}$, the probability of an error is always limited by 0.025. Use of $\hat{\delta}$ with a confidence interval is a conservative approach, which generally yields a smaller number of correct coupling directions than the analysis based on the sign of $\hat{d}$, because of the high fraction of conservative conclusions that determination of the coupling directions is impossible.

At a very low noise level ($\sqrt{2D} \le 0.03$) and a narrow confidence interval for $\hat{\delta}$, both approaches provide 100% determination of the coupling direction, a result that signifies the high reliability of a decision for a singular time series.

At a sufficiently low noise level, a series of 1000 points is long enough for reliable determination of the coupling direction. For example, at $\sqrt{2D} \le 0.06$, correct decisions were made for more than 95% of realizations. In other words, a series of length $N = 1000$ became "sufficiently long" when the value of D was reduced to approximately one-tenth of that in $\sqrt{2D} = 0.6$. It can be expected that, for $\sqrt{2D} = 0.6$, the number of points in a sufficiently long time series should be 100 times larger than N. The above considerations clarify the ideas of short and long series from the viewpoint of determining the direction of coupling. A particular value of N that divides time series into short and long depends on the noise level and on the difference $c_2^2 - c_1^2$. Examples of nonlinear analysis are presented in [8].

The new estimates are applicable to relatively short time series; however, their length should be no less than 50–100 characteristic periods. Additional numerical experiments show that it is possible to apply these estimates (the probability of an error remains predictable) to reveal weak coupling even from time series comprising 20 characteristic periods if their phase coherence coefficient ρ does not exceed 0.4. This condition automatically excludes the danger associated with phase locking of signals.

3. AN EXAMPLE FROM NEUROPHYSIOLOGY

3A. Problem Formulation and Experimental Data

An important problem in epilepsy therapy is localization of the pathological (epileptic) focus in the brain. This task is often difficult because an epileptic seizure may be caused by a pathologic brain region without noticeable tissue damage. Attempts are made to detect such regions by analyzing the dynamic behavior of electroencephalogram (EEG) signals [6, 7]. A widespread hypothesis suggests that, prior to an epileptic seizure, there occurs an increase in the influence of the pathological focus on the adjacent brain regions, thereby inducing their pathological synchronization. It seems likely that the estimation of coupling from multichannel EEG data acquired in a relatively short sliding time window can help detect changes in the character of interaction between brain regions and localize the epileptic focus.

In this study, we make an attempt to use the proposed coupling estimates for this purpose. Intracranial epileptic EEGs of a patient with temporal lobe epilepsy were supplied by Dr. R. Wennberg, Krembil Neuroscience Centre, Toronto Western Hospital, Canada. Figure 3 presents a two-channel EEG recording taken from the left temporal lobe and hippocampus with a sampling frequency of 250 Hz. It is known that the record contains an epileptic seizure and the pathological focus is located in the left temporal lobe. The start and end of the seizure are marked with the vertical dashed lines. The total recording duration is 4.5 min.

3B. Results and Discussion

The spectral analysis of the wideband EEG signals revealed several spectrum peaks at a frequency of about 2–3 Hz before and after the seizure and at 7 Hz during

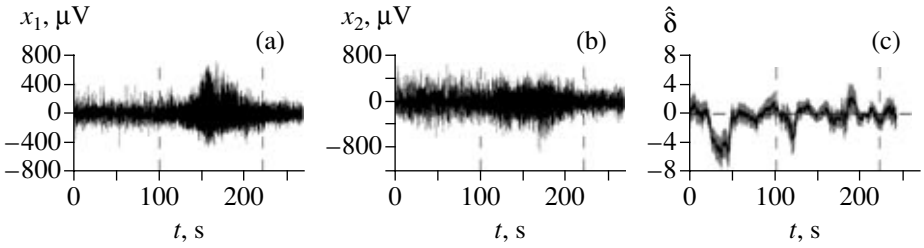

Fig. 3. Intracranial EEGs recorded from (a) the hippocampus and (b) the temporal lobe of the cortex and (c) the coupling directionality index.

the seizure. Analysis was performed using model (3) with $\tau = 0.04$ s ($100\Delta t$) and $\tau = 0.14$ s ($33\Delta t$). Phases were calculated by two methods: via bandpass filtering followed by the Hilbert transform and by wavelet transform (1) with $\omega_0 = 2$, both yielding similar results. The results of the latter approach are shown in Fig. 3. Each of the signals is plotted on time scale s corresponding to the respective peak in the scalogram (power spectrum estimate) obtained from the entire recording at $\omega_0 = 2$. For the hippocampus and cortex signals, $s = 0.44$ and 0.62 s, respectively.

The directionality index was calculated in a moving time window varying from 4 ($N = 1000$ points) to 40 s, with similar results. A change in the coupling direction is seen clearly, for example, at the window length $N = 6000$ in Fig. 3c, which presents directionality index $\hat{\delta}$ obtained with a 95% confidence interval (the gray shading). A long-term period during which the cortex's influence on the hippocampus dominates is observed about 80 s before the start of the seizure. This result is in good agreement with relevant clinical data and demonstrates the usefulness of the new coupling estimates for the localization of an epileptic focus. However, establishment of the applicability of the coupling estimates requires further investigation on a greater ensemble of EEG data. This is the goal of current investigations. (At present, the results of only three of the four EEGs taken from a patient with epileptic seizures are similar to those in Fig. 3 and no predominance of either coupling direction was found from the fourth record).

4. AN EXAMPLE FROM CLIMATOLOGY

4A. Problem Formulation and Experimental Data

The El Niño–Southern Oscillation (ENSO) and North Atlantic Oscillation (NAO) are the dominant modes of the interannual variability of climate on Earth and in the Northern Hemisphere [17, 18]. Revealing the mechanisms of their formation is of great fundamental and practical importance. Of special interest is the presence and character of the ENSO–NAO mutual coupling. Attempts to clarify the issue have been made by applying linear techniques (e.g., the method of correlation functions) to the time series of sea-surface temperature (SST) and sea-level pressure. In view of the highly intricate character of the studied processes and only short time series of reliable data from 1950 to 2004 inclusive (660 monthly average values), no reliable conclusion has been drawn about the presence of their coupling. In this study, the following climate indexes for the period 1950–2004 are analyzed:

(i) the NAO index defined as the first mode of the 500-hPa height field in the middle troposphere of the Northern Hemisphere, as derived by the rotated principle components analysis (see http://www.ncep.noaa.gov, [19], and Figs. 4a–4c);

(ii) the Niño 3.4 index characterizing SST variations in the equatorial Pacific Ocean (5°N–5°S, 170°E–120°E) (see http://www.ncep.noaa.gov and Figs. 4d–4f).

The typical time scales of interest are no shorter than two years and contain as many as 27 characteristic periods.

4B. Results and Discussion

The calculated characteristics of the NAO and Niño 3.4 indexes are shown in Fig. 4. The scalogram of the NAO index (Fig. 4b) was obtained using the Morlet transform with $\omega_0 = 6$. This smoothed power spectrum displays peaks corresponding to the time rhythms of 32 months, 108 months, etc. These peaks may be related to oscillation processes whose phases are adequately definable. The peaks of the scalogram for the Niño 3.4 index (Fig. 4e) correspond to the cycles of 12 months, 60 months, etc.

Phases were introduced with the help of the Morlet transform with $\omega_0 = 6$ and time scales s specified by the spectral peaks. The results were almost the same for ω_0 varying from 4 to 8. The coupling between each pair of the oscillation components was estimated. For both signals, the presence of coupling was concluded for the component with $s = 32$ months. Figures 4a and 4d plot the time realizations of the real part of the wavelet coefficient corresponding to $s = 32$ months (dashed lines). The phase trajectories in Figs. 4c and 4f are seen to rotate around the origin; hence, the phases are well defined.

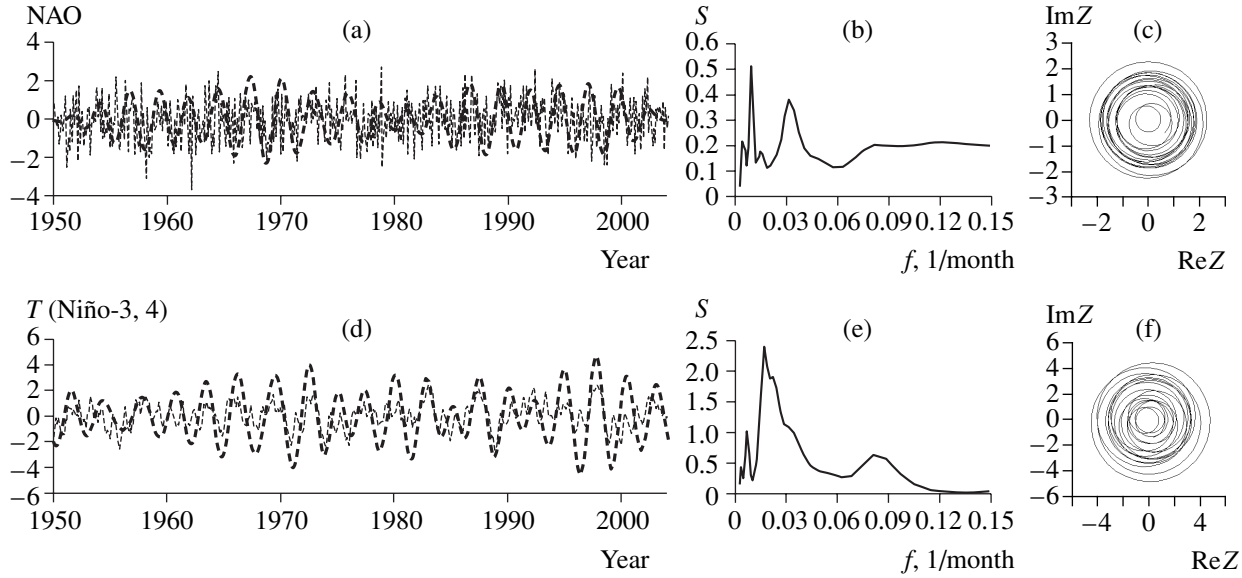

Fig. 4. Climate indexes and their characteristics: NAO (a) initial series (shadow line) and the real part of transform (1) at the scale s = 32 months (dashed line), (b) global wavelet spectrum of the signal power, and (c) a complex trajectory for the 32-month component. (d–f) The same for the Niño 3.4 index.

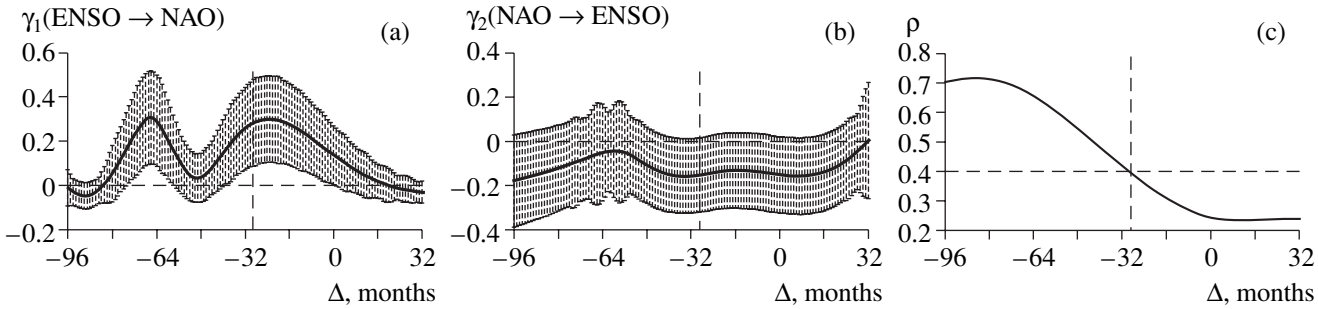

Fig. 5. Analysis of coupling between the NAO and ENSO 32-month components: (a, b) the parameters of their cross influence (solid lines, shaded lines show the 95% confidence intervals) and (c) the phase coherence factor.

In order to take into account delayed interactions [20], the models were constructed in the form

$$\varphi_{1,2}(t+\tau) - \varphi_{1,2}(t) = F(\varphi_{1,2}(t), \varphi_{2,1}(t+\Delta), \vec{a}_{1,2}) + \varepsilon_{1,2}(t), \quad (14)$$

where Δ is a supplementary model parameter, which is negative for a delayed coupling. Estimates $\gamma_{1,2}(\Delta)$ were calculated for Δ varying from a negative value of large magnitude to $\Delta = \tau$. The values $\Delta > \tau$ are physically meaningless because they imply the influence of future values on the current ones. The dependence of coefficient ρ on Δ was also calculated: $\rho(\Delta) = |\langle\exp(j(\varphi_1(t) - \varphi_2(t+\Delta)))\rangle|$. Only the values of $\gamma_{1,2}(\Delta)$ for which $\rho(\Delta) < 0.4$ were considered.

The results of applying a model in the form of (14) with τ = 32 months for the 32-month rhythms are presented in Figs. 5a and 5b. Coefficient ρ does not exceed 0.4 if $\Delta \geq -30$, and these are the only values to be considered (Figs. 5c). The estimate of the ENSO ⟶ NAO influence strength is pointwise significant within the interval $-30 < \Delta < 0$ and achieves a maximum at Δ = –24 months (Fig. 5a). With the use of additional considerations [21], the presence of the ENSO ⟶ NAO influence can be inferred with a confidence probability of 95%. This influence is most probably characterized by a delay of about 24 months, but this conclusion is not as reliable as the previous one. No signs of the inverse NAO ⟶ ENSO influence were detected (Fig. 5b).

Thus, the influence ENSO ⟶ NAO is established with a high confidence level, which is not achievable by conventional linear methods. The results of applying another nonlinear technique to solve this problem can be found in [21].

CONCLUSIONS

New estimates of the strength and directionality of coupling between two self-oscillation systems are proposed for the case of short time series. The new estimates are unbiased and supplemented with confidence intervals. They are derived rigorously under the assumptions of weak phase nonlinearity and weak coupling of the systems. However, numerical experiments demonstrate their applicability even when these assumptions are moderately violated.

The technique can be used to analyze self-oscillation systems of any kind. In particular, such estimates are useful for analyzing nonstationary signals (in biology and medicine) and insufficient experimental data (for example, in climatology). Examples of real neurophysiological and climatic processes are analyzed, and the proposed estimates are used to derive information about the coupling between cortical regions (from EEGs) and climatic processes (from series of climate indexes).

APPENDIX

Let us derive analytic expressions for variances and covariances of estimates $\hat{a}_{k,j}$ for the system of uncoupled linear oscillators described by Eqs. (2) with $G_{1,2} \equiv 0$. After the integration, equations (2) appear in the form of (7), where the values of $\varepsilon_k(t_i)$ do not depend on phases $\varphi_{1,2}(t_i)$ for any instant t_i; the values of $\varepsilon_1(t_i)$ and $\varepsilon_2(t_i)$ are independent of each other; and the process $\varepsilon_k(t_i) = \int_{t_i}^{t_i+\tau} \xi_k(t)dt$, $i = 1, 2, \ldots$, is a random Gaussian process with the zero mean and the variance $\sigma_{\varepsilon_k}^2 = 2D_k\tau$. Autocovariance function $\varepsilon_k(t_i)$ has the form

$$M[\varepsilon_k(t_i)\varepsilon_k(t_j)] = \int_{t_i}^{t_i+\tau}\int_{t_j}^{t_j+\tau} 2D_k\delta(t-t')dtdt' = \begin{cases}\sigma_{\varepsilon_k}^2(1-|t_i-t_j|/\tau), & |t_i-t_j| \le \tau \\ 0, & |t_i-t_j| > \tau.\end{cases} \quad \text{(A.1)}$$

Estimates $\hat{a}_{k,j}$ are calculated by the least squares routine. Condition (6) is represented as

$$\left\|\mathbf{A}_k\vec{\hat{a}}_k - \vec{b}_k\right\|^2 \longrightarrow \min, \quad \text{(A.2)}$$

where $\mathbf{A}_k$ is the matrix with elements $A_{i,j}^{(k)} = g_j^{(k)}(\varphi_1(t_i), \varphi_2(t_i))$, function $g_j^{(k)}(\varphi_1(t_i), \varphi_2(t_i))$ is the monomial corresponding to coefficient $a_{k,j}$ in $F(\varphi_1, \varphi_2, \vec{\hat{a}}_k)$ (see formula (4)), $\vec{b}_k$ is the vector with components $b_{k,i} = \varphi_k(t_i + \tau) - \varphi_k(t_i)$, and $\|\cdot\|$ is the Euclidean norm. The solution to problem (A.2) has the form $\vec{\hat{a}}_k = (\mathbf{A}_k^T\mathbf{A}_k)^{-1}\mathbf{A}_k^T\vec{b}_k$ [16] and can be found by solving normal equations. Assume that random matrix $\mathbf{A}_k^T\mathbf{A}_k$ is a constant matrix; i.e., $\mathbf{A}_k^T\mathbf{A}_k = M[\mathbf{A}_k^T\mathbf{A}_k] = \text{const}$. The accuracy of this assumption is determined by the time series length (N) and the sampling frequency and, in addition, numerical experiments show that it is accurate to within 5% for the considered series lengths $N \approx$ 50–100 characteristic periods with 10–20 points over the period.

With the above assumptions, it follows from the LSR theory that estimates $\vec{\hat{a}}_k$ are unbiased and obey the multidimensional Gaussian distribution. Covariance matrix $\vec{\hat{a}}_k$ has the form

$$M[\vec{\hat{a}}_k\vec{\hat{a}}_k^T] = (\mathbf{A}_k^T\mathbf{A}_k)^{-1}M[\mathbf{A}_k^T\vec{\hat{\varepsilon}}_k\vec{\hat{\varepsilon}}_k^T\mathbf{A}_k](\mathbf{A}_k^T\mathbf{A}_k)^{-1},$$

where $\vec{\hat{\varepsilon}}_k$ is the column vector with components $\varepsilon_k(t_1)$, …, $\varepsilon_k(t_N)$. The diagonal elements of matrix $M[\vec{\hat{a}}_k\vec{\hat{a}}_k^T]$ are the variances of estimates $\hat{a}_{k,j}$, and the rest of the elements are the covariances of estimates $\hat{a}_{k,i}$ and $\hat{a}_{k,j}$. Let us derive the corresponding expressions for these elements. Note that, under the above assumptions, the values of $\varphi_1(t_i)$ and $\varphi_2(t_i)$ ($i = 1, \ldots, N$) are almost uniformly distributed in the square $[0, 2\pi] \times [0, 2\pi]$. In this case, trigonometric monomials $g_j^{(k)}$ are mutually orthogonal and matrix $\mathbf{A}_k^T\mathbf{A}_k$ is diagonal (within the accepted accuracy):

$$\mathbf{A}_k^T\mathbf{A}_k = (N/2)\mathbf{I},$$

where $\mathbf{I}$ is the unit matrix.

Successive values $\varepsilon_k(t_i)$ are correlated. Using representation (A.1) and the Gaussian distribution of ξ_k and taking a number of definite integrals, we find that coefficient estimates $\hat{a}_{k,i}$ are independent and their variances are

$$\sigma_{1,i}^2 = (2\sigma_{\varepsilon_1}^2/N)\left(1 + 2\sum_{j=1}^{\tau/\Delta t-1}(1-j/N)(1-j\Delta t/\tau) \times \cos((m_i\omega_1 + n_i\omega_2)j\Delta t)\exp(-j\Delta t(m_i^2\sigma_{\varepsilon_1}^2 + n_i^2\sigma_{\varepsilon_2}^2)/2\tau)\right).$$

Replacing unknown quantities $\sigma^2_{\varepsilon_k}$ and ω_k with their estimates

$$\hat{\sigma}^2_{\varepsilon_k} = \frac{1}{N-1}\sum_{i=1}^{N}\Bigg(\varphi_k(t_i+\tau)-\varphi_k(t_i) - \frac{1}{N}\sum_{j=1}^{N}(\varphi_k(t_j+\tau)-\varphi_k(t_j))\Bigg)^2$$

and $\hat{a}_{k,1}/\tau$, respectively, and taking into account that $\tau \ll N$, we arrive at the estimate

$$\sigma^2_{1,i} = (2\hat{\sigma}^2_{\varepsilon_1}/N)\Bigg(1+2\sum_{j=1}^{\tau/\Delta t-1}(1-j\Delta t/\tau) \times \cos((m_i\hat{a}_{1,1}+n_i\hat{a}_{2,1})j\Delta t/\tau) \times \exp(-j\Delta t(m_i^2\hat{\sigma}^2_{\varepsilon_1}+n_i^2\hat{\sigma}^2_{\varepsilon_2})/2\tau)\Bigg). \quad (A.3)$$

Formula for $\hat{\sigma}^2_{2,i}$ is obtained similarly. The other variance estimates can be expressed via $\hat{\sigma}^2_{k,i}$. Specifically, variance $\hat{\sigma}^2_{\gamma_k}$ is related to the variances and covariances of $\hat{a}_{k,j}$ through (10). Since normally distributed estimates $\hat{a}_{k,i}$ and $\hat{a}_{k,j}$ are uncorrelated for $i \neq j$, estimates $\hat{a}^2_{k,i}$ and $\hat{a}^2_{k,j}$ are also statistically independent. Therefore, $\mathrm{cov}(\hat{a}^2_{k,i}, \hat{a}^2_{k,j}) = 0$ for $i \neq j$ and expression (10) is reduced to

$$\sigma^2_{\gamma_k} = \sum_j n_j^4\sigma^2_{\hat{a}^2_{k,j}}.$$

In view of the Gaussian distribution of $\hat{a}_{k,j}$, the variance of $\hat{a}^2_{k,j}$ has the form

$$\sigma^2_{\hat{a}^2_{k,j}} = 2\sigma^4_{k,j} + 4a^2_{k,j}\sigma^2_{k,j}.$$

The unbiased estimate of $\sigma^2_{\hat{a}^2_{k,j}}$ is $2\hat{\sigma}^4_{k,j} + 4(\hat{a}^2_{k,j} - \hat{\sigma}^2_{k,j})\hat{\sigma}^2_{k,j}$. However, it often takes very small or even negative values, a phenomenon that may lead to an erroneous interpretation of the significance level obtained for $\hat{a}^2_{k,j}$. Hence, it is better to use the overvalued estimate

$$\hat{\sigma}^2_{\hat{a}^2_{k,j}} = \begin{cases} 2\hat{\sigma}^4_{k,j} + 4(\hat{a}^2_{k,j} - \hat{\sigma}^2_{k,j})\hat{\sigma}^2_{k,j}, & \hat{a}^2_{k,j} - \hat{\sigma}^2_{k,j} \geq 0 \\ 2\hat{\sigma}^4_{k,j}, & \hat{a}^2_{k,j} - \hat{\sigma}^2_{k,j} < 0. \end{cases}$$

Finally, the estimate for $\sigma^2_{\gamma_k}$ can be taken as

$$\hat{\sigma}^2_{\gamma_k} = \begin{cases} \sum_j n_j^4\hat{\sigma}^2_{\hat{a}^2_{k,j}}, & \gamma_k > 5\sum_j n_j^4\hat{\sigma}^2_{\hat{a}^2_{k,j}} \\ (1/2)\sum_j n_j^4\hat{\sigma}^2_{\hat{a}^2_{k,j}}, & \gamma_k \leq 5\sum_j n_j^4\hat{\sigma}^2_{\hat{a}^2_{k,j}}. \end{cases} \quad (A.4)$$

This construction stems from the following considerations. At large values of c_k, the first formula in (A.4) yields a good estimate. At $c_k \approx 0$, this estimate is on average twice as large as the true value (according to our numerical experiments) and, hence, must be halved. Such a combined estimation is an acceptable trade-off for all cases. The variance estimates thus obtained are used to derive semiempirical formulas for the confidence intervals of $c^2_{1,2}$ and δ (see Section 2A).

ACKNOWLEDGMENTS

The author thanks B.P. Bezruchko, I.I. Mokhov, M.B. Bodrov, R. Wennberg, and J.L. Perez Velazquez for cooperation and valuable discussions.

This study was supported by the Basic Research and Higher Education (BRHE) program, grant no. REC–006; the Russian Foundation for Basic Research, project no. 05-02-16305; and the Russian Science Support Foundation.

REFERENCES

1. B. Bezruchko, V. Ponomarenko, M. G. Rosenblum, and A. S. Pikovsky, Chaos **13**, 179 (2003).
2. S. Jevrejeva, J. Moore, and A. Grinsted, J. Geophys. Res. **108**, 4677 (2003).
3. N. B. Janson, A. G. Balanov, V. S. Anishchenko and P. V. E. McClintock, Phys. Rev. Lett. **86** (9), 1749 (2001).
4. M. G. Rosenblum, L. Cimponeriu, A. Bezerianos et al., Phys. Rev. E **65**, 041909 (2002).
5. M. D. Prokhorov, M. B. Bodrov, V. I. Ponomarenko, et al., Biofizika **50**, 914 (2005).
6. J. Arnhold, K. Lehnertz, P. Grassberger, and C. E. Elger, Phys. D (Amsterdam) **134**, 419 (1999).
7. F. Mormann, K. Lehnertz, P. David and C. E. Elger, Phys. D (Amsterdam) **144**, 358 (2000).

8. D. A. Smirnov, M. B. Bodrov, J. L. Perez Velazquez, et al., Chaos **15**, 024102 (2005).
9. M. G. Rosenblum and A. S. Pilovsky, Phys. Rev. E **64**, 045202 (2001).
10. D. A. Smirnov and B. P. Bezruchko, Phys. Rev. E **68**, 046209 (2003).
11. A. S. Pikovskii, M. G. Rozenblyum, and J. Kurths, *Synchronization: A Fundamental Nonlinear Phenomenon* (Tekhnosfera, Moscow, 2003) [in Russian].
12. M. G. Rosenblum, A. S. Pikovsky, J. Kurths, et al., in *Neuro-Informatics*, Ed. by F. Moss and S. N. Y. Gielen (Elsevier Sci., New York, 2000), p. 279.
13. J. P. Lachaux, E. Rodriguez, M. Le Van Quyen, et al., Int. J. Bifurcations Chaos Appl. Sci. Eng. **10**, 2429 (2000).
14. C. Torrens and G. P. Compo, Bulletin American Meteorological Society **79** (1), 61 (1998).
15. A. S. Pikovsky, M. G. Rosenblum, and J. Kurths, Int. J. Bifurcations Chaos Appl. Sci. Eng. **10**, 2291 (2000).
16. G. A. F. Seber, *Linear Regression Analysis* (Wiley, New York, 1977; Mir, Moscow, 1980).
17. J. W. Hurrell and H. van Loon, Climatic Change **36** (3–4), 301 (1997).
18. I. I. Mokhov, A. V. Eliseev, and D. V. Khvorost'yanov, Izv. Akad. Nauk, Fiz. Atmos. Okeana **36**, 741 (2000).
19. A. G. Barnston and R. E. Livezey, Mon. Weather Rev. **115**, 1083 (1987).
20. L. Cimponeriu, M. Rosenblum, and A. Pikovsky, Phys. Rev. E **70**, 046213 (2004).
21. D. A. Smirnov and I. I. Mokhov, *Topical Problems of Nonlinear Wave Physics (Int. Symp.: Plenary Talks and Workshops, St. Petersburg–Nizhni Novgorod, Russia, 2–9 August, 2005)* (Institute of Applied Physics, Nizhni Novgorod, 2005), p. 46.